Molecular Immunology 116 (2019) 191–198

Contents lists available at ScienceDirect

Molecular Immunology

journal homepage: www.elsevier.com/locate/molimm

Curcumin inhibits proliferation and soluble collagen synthesis of NIH/3T3 cell line by modulation of miR-29a and via ERK1/2 and β-catenin pathways

Jianhua Zhang[a], Mei Song[b], Weifeng Li[a], Feng Zhao[a,*], Yuguo Li[c,*]

[a] Department of Burn and Plastic Surgery, Linyi People's Hospital, Linyi 276003, Shandong, China
[b] Department of Endocrinology, Linyi People's Hospital, Linyi 276003, Shandong, China
[c] Department of Orthopaedics, Lanling County People's Hospital, Linyi 277799, Shandong, China

ARTICLE INFO

Keywords:
Scars
TGFβ1
Curcumin
miR-29a

ABSTRACT

Background: Scars affects the appearance and results in tissue damage. In this research, we preliminarily studied the function and mechanism of curcumin (CUR) on cell proliferation and soluble collagen synthesis in NIH-3T3 cells.

Methods: CCK-8 was used to detect the IC50 of CUR. Moreover, Western blot was used to measure the expression of cell proliferation-related, soluble collagen synthesis and pathway-related proteins. Sircol assay was determined the expression of soluble collagen. Furthermore, reverse transcription quantitative PCR (RT-qPCR) was used to determined miR-29a, α-smooth muscle aorta (α-SMA), soluble collagen 1 (Col 1) and Col 3 expression.

Results: CUR inhibited cell viability and proliferation-related proteins expression. Transforming growth factor-β (TGFβ1)-induced heightened the expression of proliferation-related proteins and soluble collagen synthesis-related proteins. CUR inhibited TGFβ1-induced proliferation and soluble collagen synthesis. Furthermore, CUR positively related miR-29a and miR-29a mimic inhibited TGFβ1-induced proliferation and soluble collagen synthesis. Besides, transfection with miR-29a inhibitor could partly reverse the effects of CUR. CUR inhibited the ERK1/2 and β-catenin pathways and the miR-29a inhibitor reversed the above results. Otherwise, soluble collagen 1 (Col 1) partly reversed the effects of CUR on proliferation and soluble collagen synthesis and silenced Col 1/3 could inhibit ERK1/2 and β-catenin signaling pathways.

Conclusion: CUR restrained TGFβ1-induced proliferation and soluble collagen synthesis in NIH-3T3 cells by up-regulation of miR-29a via ERK1/2 and β-catenin signaling pathways.

1. Introduction

Scars is called by a joint name for the facade and histopathological variations of skin when skin is damaged by trauma, cut wounds, burns and so on (desJardins-Park et al., 2019). Scars not only affect the facade, but also cause dysfunction. This is bringing vastly pain to the patient. Current studies had verified that the formation of scars was strongly associated with the excessive proliferation of fibroblasts. It was stated that the direct cause of scars was the unusual accumulation of extracellular matrix (A. Xiao and Ettefagh, 2019). In this process, fibroblasts play a key role. Fibroblasts firsthandly synthesize α-smooth muscle aorta (α-SMA), soluble collagen 1 (Col 1) and soluble collagen 3 (Col 3) and form extracellular matrix, followed by releasing transforming growth factor-β (TGFβ1) which is capable of controlling the metabolism of extracellular matrix (Carswell and Borger, 2019). At present, the drugs for treating scars include glucocorticoids, antihistamines, immunesuppressive agents and so on, but there are numerous disadvantages such as recurrence, side effects, and long-term administration (Ogawa, 2019). Therefore, it is particularly vital to screen safer and more effective drugs from natural drugs.

Curcumin (CUR) is a polyphenolic substance extracted from the traditional Chinese medicine turmeric. Its main functions are elimination of inflammation, inhibition of tumors, and anti-fibrosis (Yuan et al., 2019). Studies *in vitro* and *in vivo* had confirmed the role of CUR in scars (Bondan et al., 2017; Yuan et al., 2017, 2015). It had found that CUR could promote wound healing in rabbit (Jia et al., 2014). Further study found that CUR could significantly control fibroblast proliferation and soluble collagen synthesis and they constructed a model of scars disease (Saidi et al., 2019). This model was used for reference in this experiment. Moreover, literatures displayed CUR restrained tumor progress by microRNAs (miRNAs) (Zhou et al., 2017).

miRNA is a non-coding RNA of approximately 21–25 nt in size. In

* Corresponding authors.
E-mail addresses: zhao0163zf@sina.com (F. Zhao), liyuguo111@163.com (Y. Li).

https://doi.org/10.1016/j.molimm.2019.10.018
Received 26 June 2019; Received in revised form 4 September 2019; Accepted 23 October 2019
Available online 08 November 2019
0161-5890/

recent years, the regulation of miRNAs involved in skin wound repair had been widely proven (Zhang et al., 2018; Zhao et al., 2018aa; Zhao et al., 2018bb). miR-29a is one of the miRNAs that can regulate this process. It can accelerate fibroblast migration (Tu et al., 2018). miR-29a had been shown to play an vital part in scars (L. Xiao et al., 2017), so study miR-29a may be a potential treatment option.

In this experiment, NIH/3T3 cells were used as the experimental object to investigate the therapeutic function of CUR on scars *in vitro*. We observed the functions of CUR and miR-29a on the cell proliferation and soluble collagen synthesis in scars and explored the possible mechanism of action of CUR on scars. In this paper, the basic research about CUR provided a new basis for the clinical treatment of scars.

2. Materials and methods

2.1. Cell culture and treatment

NIH-3T3 cells (China Center for Type Culture Collection, CCTCC, Wuhan, China) were cultured in Dulbecco's modified Eagle medium (DMEM, Gibco, Grand Island, NY, US). The medium containing 10 % fetal bovine serum (FBS, Gibco) 100 U/mL penicillin (Beyotime, Haimen, China) and 100 μg/mL streptomycin (Beyotime) at 5 % CO_2, 37 °C. The culture medium was replaced every two day. CUR (Sigma, St. Louis, US) was diluted with DMSO in 10 mM, immediately after, diluted to DMEM at a concentration of 0–10 μM. The dosing time was 12 h. TGFβ1 (Abcam, Cambridge, UK) was reconstituted with ddH_2O, 0.1 % BSA (Beyotime) to 10 ng/mL and the processing time is 24 h. Col 1 were purchased from Advanced Biomatrix (San Diego, CA, US) and reconstituted with 0.1 M acetate solution to 10 μg/mL according to instruction.

2.2. CCK-8 assay

Cells were inoculated in 96-well plates (Beyotime) at a 5×10^3 cells/well. After the dosing treatment, the CCK-8 solution (Bioswamp, Wuhan, China) was added to the medium according to the instructions, the plates were incubated 1 h in the dark at 5 % CO_2, 37 °C. The absorbance was quantitated by microplate reader (Bio-Rad Labs, Sunnyvale, US) at 450 nm.

2.3. Reverse transcription quantitative PCR (RT-qPCR)

Trizol was used to extract RNA (Molecular Research Center, Cincinnati, Ohio). The Taqman MicroRNA Reverse Transcription Kit (Thermo Fisher Scientific, Runcorn, UK) and Taqman Universal Master Mix II within TaqMan MicroRNA Assay of miR-29a and U6 (Thermo Fisher Scientific) were used for detecting miR-29a expression. RNA PCR Kit (AMV) Ver.3.0 (TaKaRa Biotechnology, Dalian, China) was used for the test the RNA expression of α-SMA, Col 1, Col 3. Samples were run in triplicate. The $2_{-\Delta\Delta Ct}$ equation was used to quantify the data.

2.4. Transfection

The miR-29a inhibitor, NC inhibitor, si-Col1, si-Col3 and si-NC were synthesized by GenePharma Co. (Shanghai, China). Lipofectamine 3000 (Carlsbad Life Technologies, Carlsbad, US) was used on cell transfection. The transfection efficiency was evaluated by qRT-PCR.

2.5. Measurement of soluble collagen protein

The expression of soluble collagens in culture supernatants were measured by sircol assay kit (Biocolor, Newtonabbey, UK). Samples were run in duplicate and average it.

2.6. Western bolt

Proteins were extracted from cells by RIPA lysis buffer (Beyotime) plus protease inhibitor (Beyotime). We used protein assay kit (Bioswamp) quantified the proteins. This experiment was established by using the Bio-Rad system. Primary antibodies contained anti-VEGF antibody (ab1316, Abcam), anti-CyclinD1 antibody (ab16663, Abcam), anti-CDK1 antibody (ab131450, Abcam), anti-β-actin antibody (ab8227, Abcam), anti-α-SMA (ab32575, Abcam), anti-Col 1 antibody (ab34710, Abcam), anti-Col 3 antibody (ab7778, Abcam), anti-ERK1 + ERK2 antibody (ab184699, Abcam), anti-ERK1 (phospho T202) + ERK2 (phospho T185) antibody (ab201015, Abcam), anti-β-catenin antibody (ab32572, Abcam). Primary antibodies were prepared at a dilution of 1:1000 in 5 % blocking buffer. The primary antibodies were cultured at 4 °C overnight, washed and incubated with secondary antibodies goat anti-rabbit IgG (ab6721, Abcam, 1:5000) 1 h at 25 °C. After rinsing, the polyvinylidene fluoride (PVDF) membrane bring the antibody were shifted to system. Finally, added 200 μL HRP substrate (Millipore Corp., Billerica, US) to the surface. Captured signal and quantified by Image Lab™ Software (Bio-Rad). The above experiments were used β-actin as internal parameters.

2.7. Statistical analysis

All experiments were repeated three times. Data were expressed as mean ± Standard Deviation (SD). Statistical analyses were performed by using Graph pad 6.0 (Graph Pad Software, CA, US). The *P*-values were calculated using a one-way analysis of variance (ANOVA) and *t* test. $P < 0.05$ was considered statistically significant.

3. Results

3.1. CUR inhibited proliferation of NIH-3T3 cells

Firstly, after CUR therapy, the viability of NIH-3T3 cells was detected. The results presented CUR statistically depressed the viability of NIH-3T3 cells at a dose-dependent method (Fig. 1A, $P < 0.05$, $P < 0.01$ or $P < 0.001$). The IC50 was 6.026 ± 0.276 μM. Therefore, the 6 μM and 8 μM CUR was respectively used for next experiments. The Western bolt results (Fig. 1B and 1C) showed that the expression of proliferation associated proteins VEGF ($P < 0.001$), Cyclin D1 ($P < 0.01$) and CDK4 ($P < 0.001$) were significantly descended after the addition of the 6 μM and 8 μM CUR.

3.2. CUR inhibited soluble collagen synthesis in NIH-3T3 cells

Firstly, we treated NIH-3T3 cells with TGFβ1 (10 ng/mL) and TGFβ1 + CUR (6 μM and 8 μM) for 24 h. The results found that the amount of soluble collagens were meaningfully increased when adding TGFβ1 (Fig. 2A, $P < 0.001$) and both 6 μM and 8 μM CUR inhibited the above phenomenon (Fig. 2A, $P < 0.05$). The results of qRT-PCR (Fig. 2B) displayed that CUR (6 μM or 8 μM) inhibited the expression of α-SMA ($P < 0.01$), Col 1($P < 0.01$) and Col 3 ($P < 0.05$ or $P < 0.01$) which were caused by TGF-β1 and Western bolt (Fig. 2C and 2D) displayed that CUR (6 μM) inhibited the TGF-β1-induced expression of α-SMA ($P < 0.01$), Col 1($P < 0.01$) and Col 3 ($P < 0.001$).

3.3. CUR up-regulated miR-29a in NIH-3T3 cells

Many studies displayed CUR worked in disease through miRNAs (Zhou et al., 2017), so we further investigated whether CUR can regulate miR-29a. The expression of miR-29a was tested by qRT-PCR in NIH-3T3 cells after 6 μM or 8 μM CUR treatments. The CUR meaningfully boosted the expression of miR-29a in NIH-3T3 cells (Fig. 3, $P < 0.01$ or $P < 0.001$).

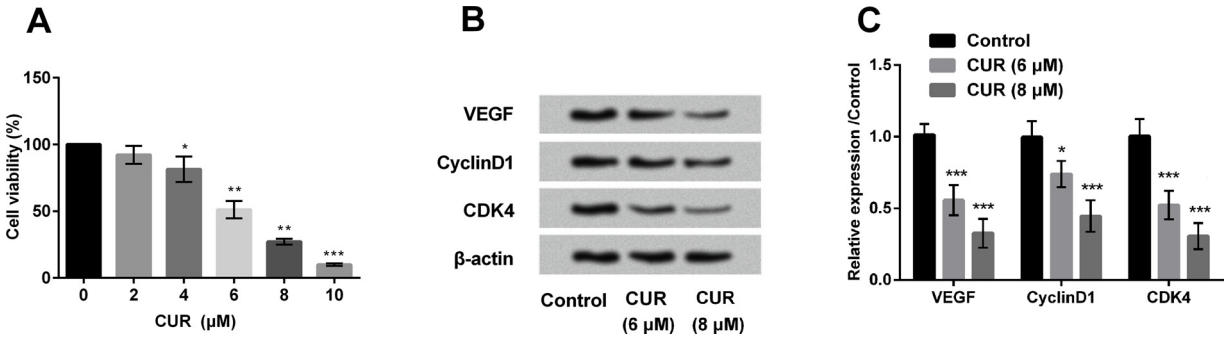

Fig. 1. Curcumin (CUR) inhibited proliferation of NIH-3T3 cells.
(A) After CUR therapy, the viability of NIH-3T3 cells was detected. The results presented CUR statistically depressed the viability of NIH-3T3 cells at a dose-dependent method. The IC50 was 6.026 ± 0.276 μM. (B and C) The results showed that the expression of vascular endothelial growth factor (VEGF), Cyclin D1 and cyclin-dependent kinases 4 (CDK4) were meaningfully descended after 6 μM and 8 μM CUR treatment. (* $P < 0.05$; ** $P < 0.01$; *** $P < 0.001$).

3.4. miR-29a mimic inhibited cell proliferation and CUR-induced soluble collagen synthesis

Firstly, miR-29a mimic statistically enhanced miR-29a expression (Fig. 4A, $P < 0.001$). Further results showed that miR-29a mimic reduced the expression of VEGF, Cyclin D1 and CDK4 (Fig. 4B and 4C, $P < 0.05$ or $P < 0.01$). Then we explored the impact of miR-29a mimic on soluble collagen synthesis. The results displayed that miR-29a

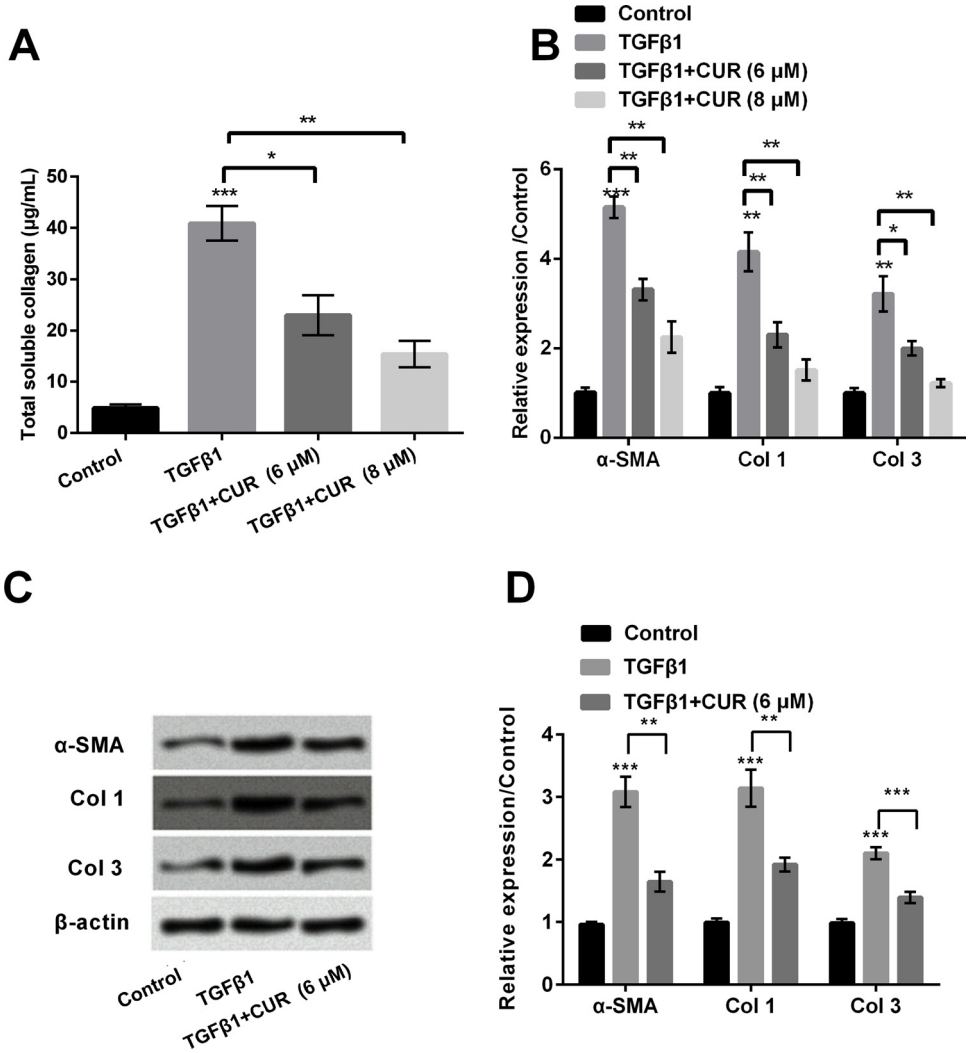

Fig. 2. Curcumin (CUR) inhibited soluble collagen synthesis in NIH-3T3 cells.
(A) CUR (6 μM and 8 μM) restrained the transforming growth factor-β1 (TGF-β1)-induced rise of soluble collagen expression. (B) Reverse transcription quantitative PCR (RT-qPCR) result discovered CUR (6 μM and 8 μM) restrained the expression of α-smooth muscle aorta (α-SMA), soluble collagen 1 (Col 1) and soluble collagen 3 (Col 3) which were enhanced by TGF-β1. (C and D) western blot result discovered CUR (6 μM) restrained the TGF-β1-induced expression of α-SMA, Col 1 and Col 3. (* $P < 0.05$; ** $P < 0.01$; *** $P < 0.001$).

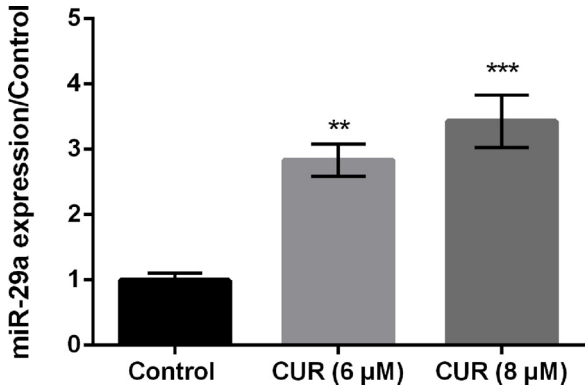

Fig. 3. Curcumin (CUR, 6 μM and 8 μM) promoted the expression of miR-29a in NIH-3T3 cells. (** $P < 0.01$).

mimic can meaningfully decline the TGFβ1-induced expressions of soluble collagen (Fig. 4D, $P < 0.05$), α-SMA, Col 1 and Col 3 (Fig. 4E and 4 F, $P < 0.01$).

3.5. miR-29a inhibitor reversed the CUR-induced inhibition on cell proliferation and soluble collagen synthesis

Based on the results of Fig. 4, we found that miR-29a inhibitor statistically reduced miR-29a expression (Fig. 5A, $P < 0.01$). Further results showed that miR-29a inhibitor alleviated the 6 μM CUR-reduced cell viability. (Fig. 5B, $P < 0.01$) and the expression of VEGF (Fig. 5C and 5D, $P < 0.01$), Cyclin D1 and CDK4 (Fig. 5C and 5D, $P < 0.001$). Then we explored the impact of miR-29a inhibitor on soluble collagen synthesis. The results of western blot (Fig. 5E and 5 F) and qRT-PCR (Fig. 5G) displayed that miR-29a inhibitor can meaningfully enhance the amount of α-SMA ($P < 0.01$), Col 1 ($P < 0.01$ or $P < 0.001$) and Col 3 ($P < 0.05$ or $P < 0.01$) which was inhibited by 6 μM CUR. On the other hand, the sircol assay results showed the same trend (Fig. 5H, $P < 0.05$). In general, CUR inhibited cell proliferation and soluble collagen synthesis by up-regulating miR-29a.

3.6. CUR and miR-29a were involved in ERK1/2 and β-catenin signaling pathways

From Fig. 6A and B, we can see that 6 μM CUR inhibited the ratio of p/t-ERK1/2 and the expression of β-catenin ($P < 0.001$). After the system was treated with miR-29a inhibitor, the ratio of p/t-ERK1/2 (Fig. 6A, $P < 0.001$) and the expression of β-catenin (Fig. 6B, $P < 0.001$) were increased. Otherwise, we discovered miR-29a mimic declined the ratio of p/t-ERK1/2 (Fig. 6C, $P < 0.01$) and the expression of β-catenin (Fig. 6D, $P < 0.01$). These results indicated that CUR and miR-29a were involved in ERK1/2 and β-catenin signaling pathways.

3.7. Col 1 remitted the CUR-induced inhibition on cell proliferation, soluble collagen synthesis and pathways

Col 1 enhanced the 6 μM CUR-induced decrease in cell viability (Fig. 7A, $P < 0.05$) and the expression of soluble collagen (Fig. 7B, $P < 0.001$). Then we explored the impact of Col 1 on cell pathways and displayed Col 1 enhanced the ratio of p/t-ERK1/2 and the expression of β-catenin (Fig. 7C and 7D, $P < 0.001$) which was caused by CUR. These results indicated that Col 1 remitted the CUR-induced inhibition on cell proliferation, soluble collagen synthesis and pathways.

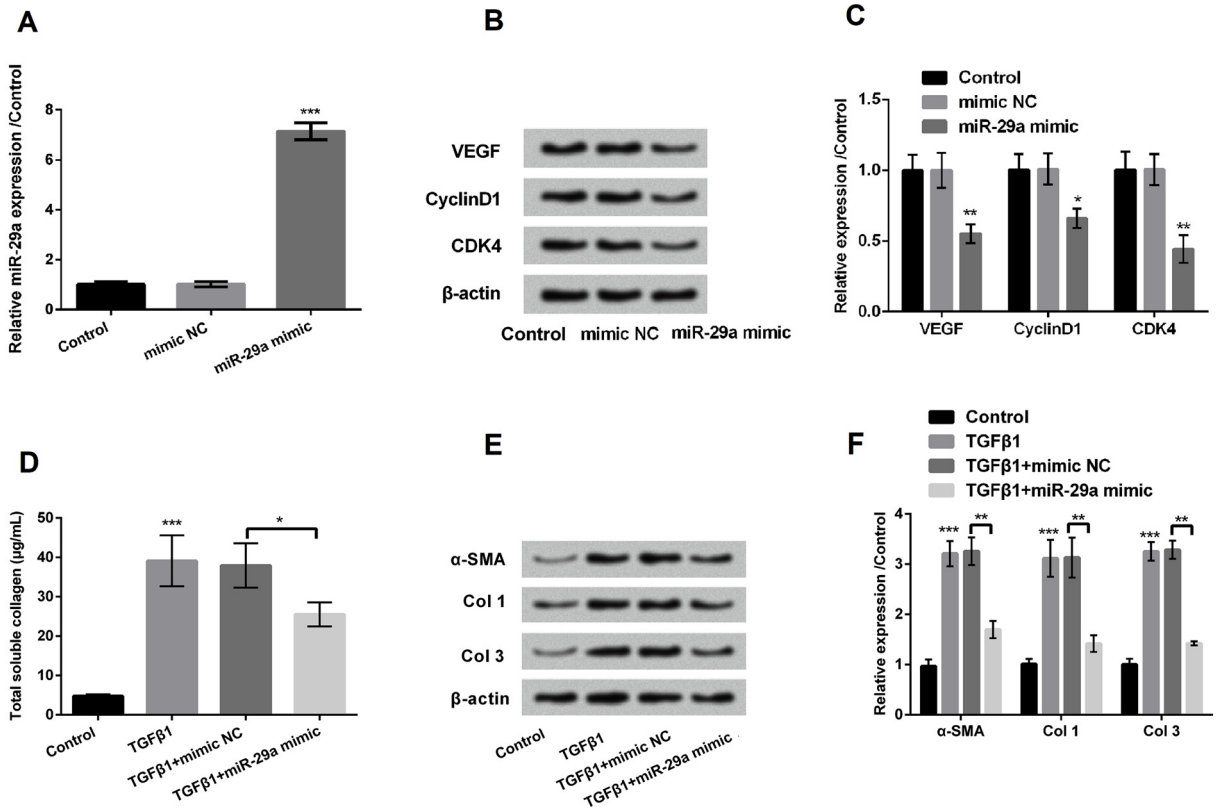

Fig. 4. miR-29a mimic inhibited cell proliferation and CUR-induced soluble collagen synthesis.
(A) miR-29a mimic statistically enhanced miR-29a expression. (B and C) miR-29a mimic reduced the expression of VEGF, Cyclin D1 and CDK4. miR-29a mimic can meaningfully decline the TGFβ1-induced expressions of (D) soluble collagen, (E and F) α-SMA, Col 1 and Col 3. (* $P < 0.05$; ** $P < 0.01$; *** $P < 0.001$).

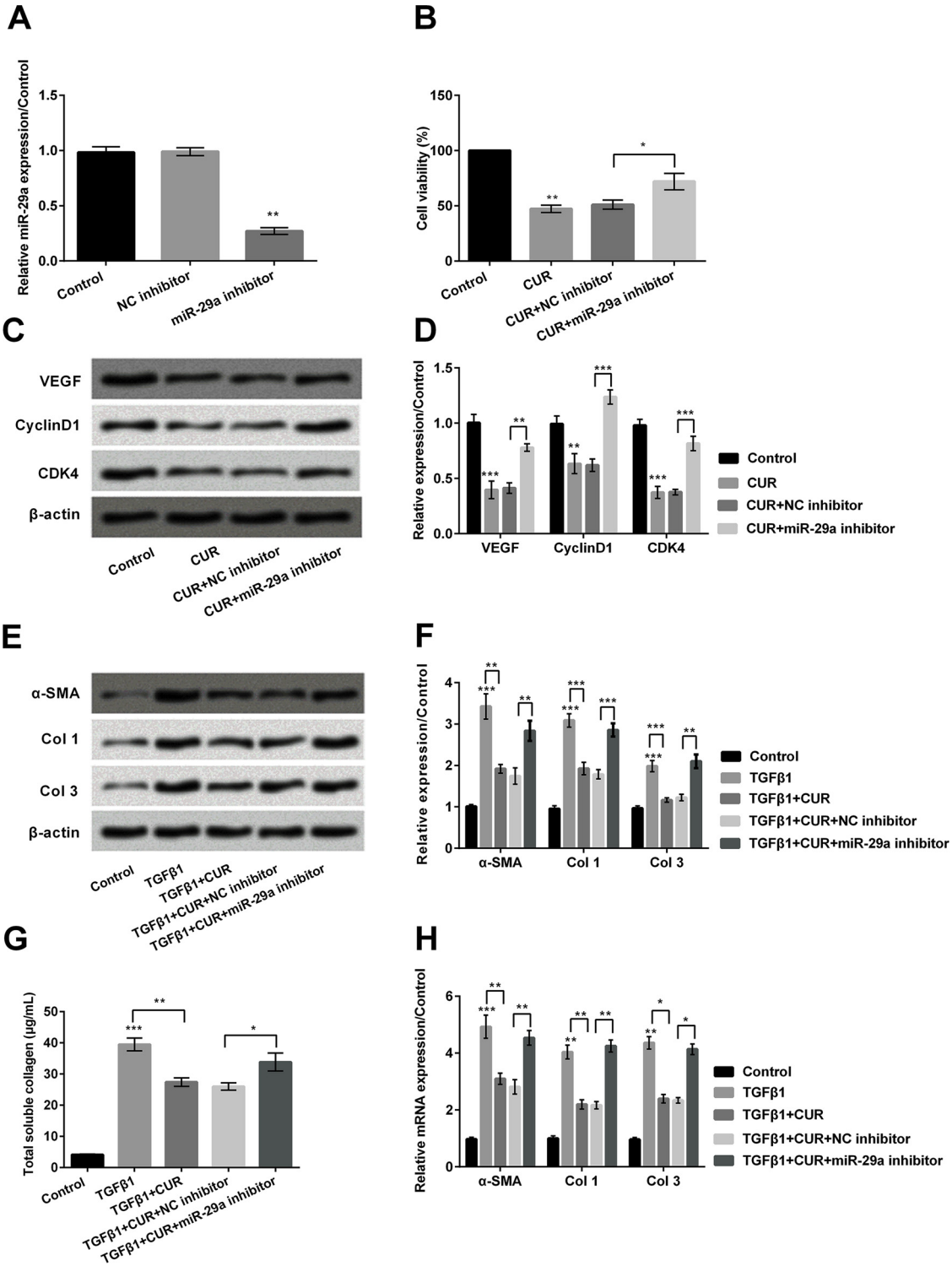

Fig. 5. miR-29a inhibitor reversed the curcumin (CUR)-induced inhibition on cell proliferation and soluble collagen synthesis.
(A) The expression of miR-29a was significantly reduced compared to NC inhibitor when treated with miR-29a inhibitor. (B) miR-29a inhibitor significantly enhanced the CUR-induced cell viability. (C and D) The expression of vascular endothelial growth factor (VEGF), Cyclin D1 and cyclin-dependent kinases 4 (CDK4) were declined after adding CUR, and this proliferation were alleviated when miR-29a inhibitor transfected to the system. (E and F and G and H) The expression of α-smooth muscle aorta (α-SMA), soluble collagen 1 (Col 1) and soluble collagen 3 (Col 3) were declined after adding CUR, and this soluble collagen synthesis were alleviated when miR-29a inhibitor transfected to the system. (* $P < 0.05$; ** $P < 0.01$; *** $P < 0.001$).

3.8. Silenced Col 1 and Col 3 inhibited ERK1/2 and β-catenin signaling pathways

When transfected si-Col 1 into cells (Fig. 8A, $P < 0.01$), the Col 1 expression were meaningfully declined. Besides, the ratio of p/t-ERK1/2 and the expression of β-catenin were declined (Fig. 8B and 8C, $P < 0.01$ or $P < 0.001$). Meanwhile, si-Col 3 declined the Col 3 expression (Fig. 8D, $P < 0.01$) and also declined the ratio of p/t-ERK1/2 and the expression of β-catenin (Fig. 8B and 8C, $P < 0.01$). These results indicated silenced Col 1 and Col 3 inhibited ERK1/2 and β-catenin

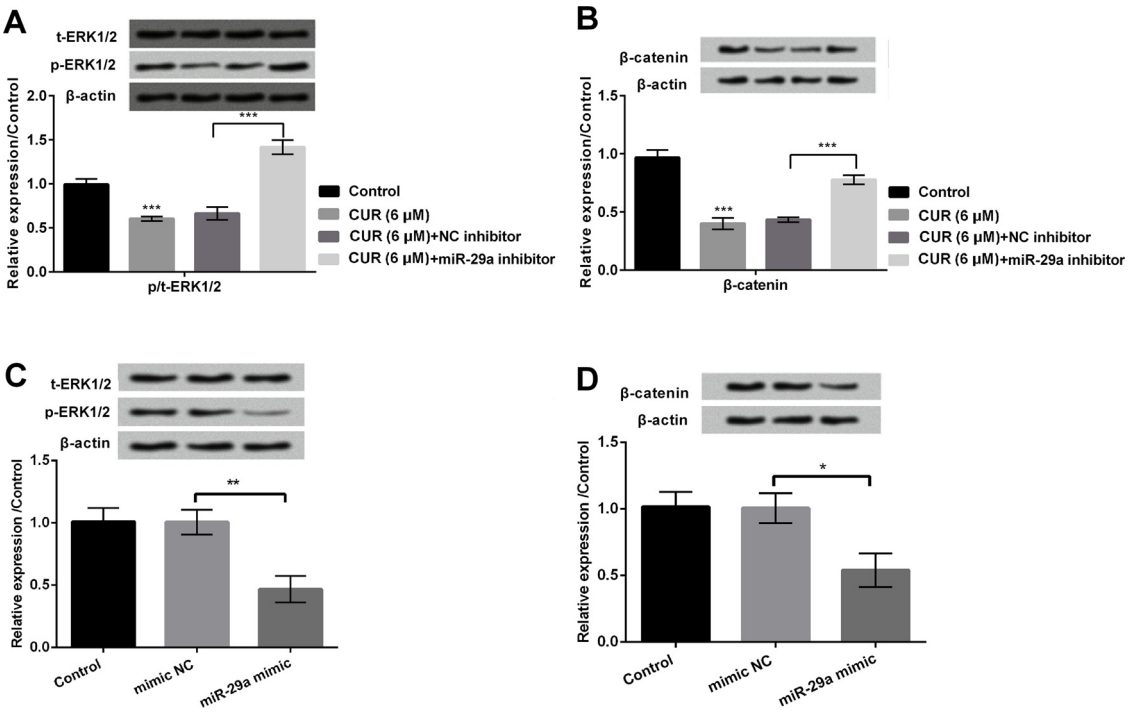

Fig. 6. Curcumin (CUR) and miR-29a were involved in ERK1/2 and β-catenin signaling pathways.
(A) CUR (6 μM) inhibited (A) the ratio of p/t-ERK1/2 and (B) the expression of β-catenin. miR-29a inhibitor increased the ratio of p/t-ERK1/2 and the expression of β-catenin. Otherwise, miR-29a mimic declined (C) the ratio of p/t-ERK1/2 and (D) the expression of β-catenin. (* $P < 0.05$; ** $P < 0.01$; *** $P < 0.001$).

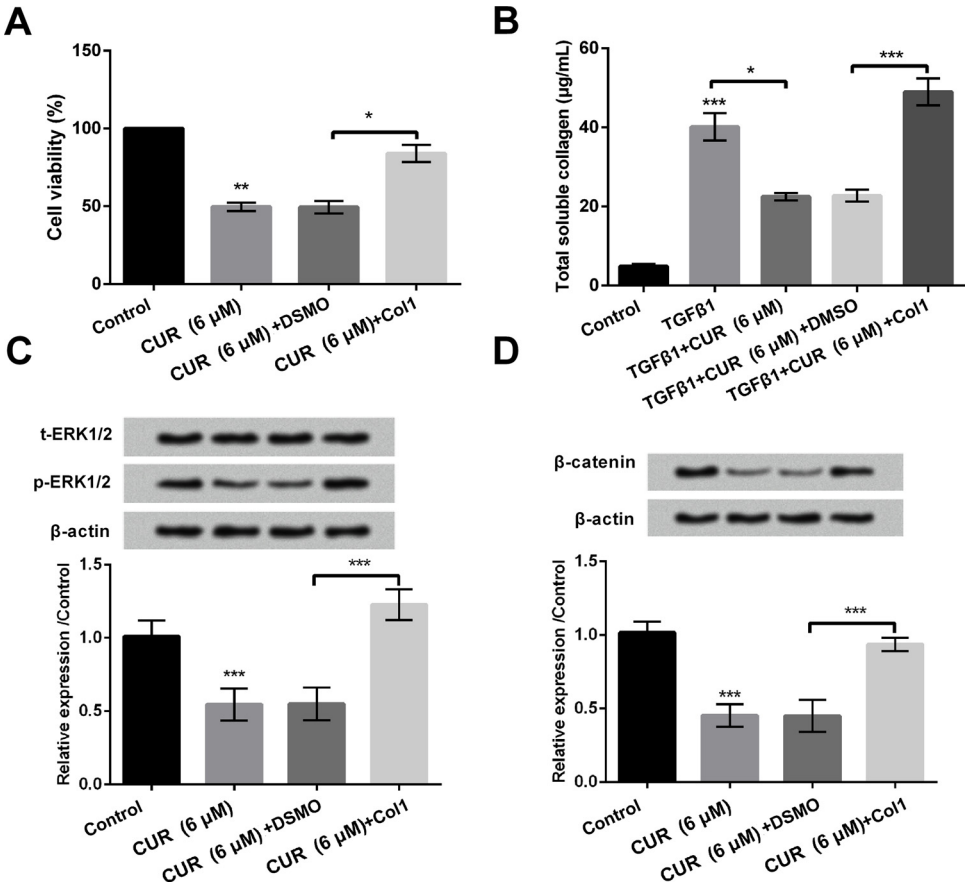

Fig. 7. Soluble collagen 1 (Col 1) remitted the curcumin (CUR)-induced inhibition on cell proliferation, soluble collagen synthesis and pathways.
(A) Col 1 enhanced the 6 μM CUR-induced decrease in cell viability and (B) the expression of soluble collagen. Then, Col 1 enhanced the ratio of (C) p/t-ERK1/2 and (D) the expression of β-catenin. (* $P < 0.05$; *** $P < 0.001$).

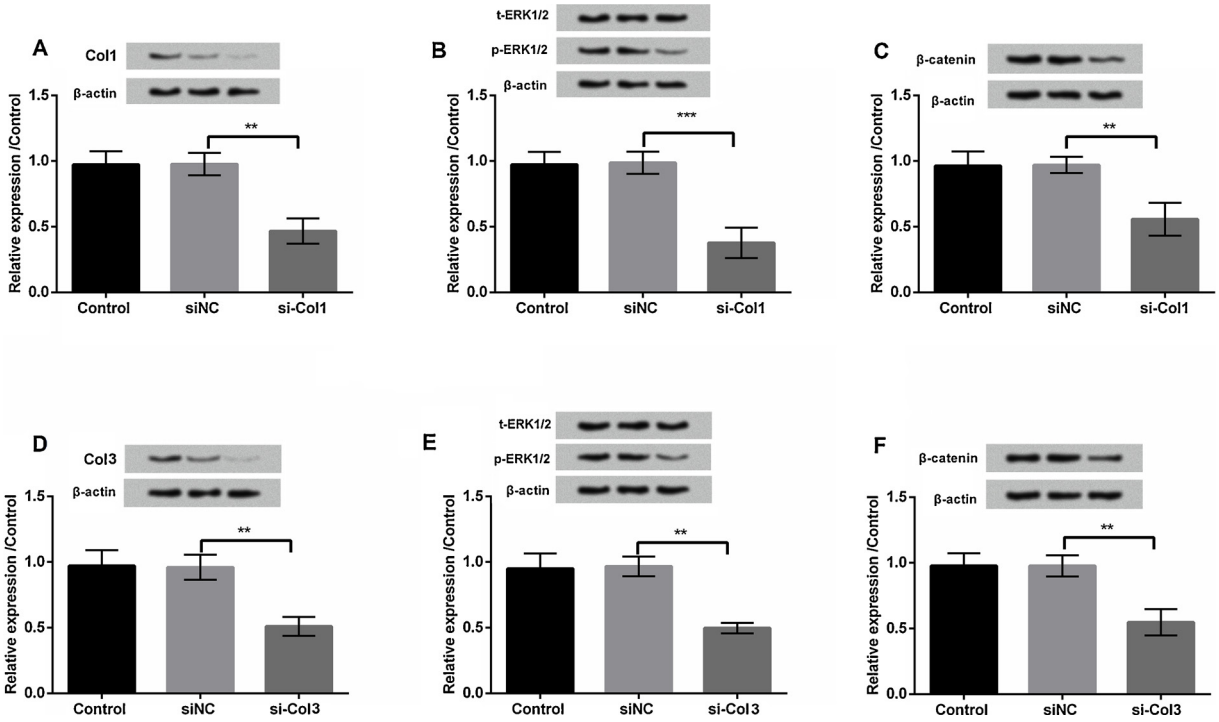

Fig. 8. Silenced soluble collagen (Col) 1 and Col 3 inhibited ERK1/2 and β-catenin signaling pathways.
(A) si-Col 1 meaningfully declined Col 1 expression. Besides, it declined (B) the ratio of p/t-ERK1/2 and (C) the expression of β-catenin. Meanwhile, (D) si-Col 3 declined the Col 3 expression and also declined (E) the ratio of p/t-ERK1/2 and (F) the expression of β-catenin. (** $P < 0.01$; *** $P < 0.001$).

signaling pathways.

4. Discussion

Scars are the result of abnormal body recovery after skin damage. Its breaks the appearance and causes tissue damage at the same time (Gauglitz et al., 2018). In this experiment, we were taking NIH-3T3 cells as research objects and different concentrations of CUR were used to investigate the CUR functions. TGFβ1 acted on NIH-3T3 cells, and it was displayed that TGFβ1 significantly controlled soluble collagen synthesis. This indicated that we had successfully constructed a model of scars disease. Next, through the observation of VEGF, Cyclin D1, CDK4, Col 1, Col 3 and α-SMA expression, we explored the resistance to scars effect of CUR in cell proliferation and soluble collagen synthesis. In addition, we also found that miR-29a was up-regulated after the addition of CUR. Then we are surprised to find that CUR exhibited suppressive effects on cell proliferation and soluble collagen synthesis. miR-29a and Col were involved the CUR-induced inhibition on cell proliferation, soluble collagen synthesis and pathways. Although the pronounced pathogenesis of scars remains unclear, TGFβ is currently thought to be the major profibrotic growth factor (Lichtman et al., 2016). TGFβ has three different isomers. Among them, TGFβ1 is the most critical pathogenic factor of scars (Al-Qattan et al., 2018). TGFβ1 is highly expressed in scars tissue and fibroblasts, and fibroblasts are very subtle to TGF-β1. TGFβ1 in scars principally accelerates fibrosis by stimulating fibroblast proliferation and enhancing soluble collagen synthesis (Han et al., 2019; Zhao et al., 2018aa; Zhao et al., 2018bb). Our research also proved this. When adding TGFβ1 to NIH-3T3 cells, the levels of soluble collagens, α-SMA, Col 1 and Col 3 were meaningfully increased.

CUR is taken from the dried stem of the herbaceous turmeric, and its medicinal properties are mild. Initially, it was used as spices and pigment (Lelli et al., 2017). Recently, as its anti-inflammatory (Vecchi Brumatti et al., 2014), anti-cancer (Devassy et al., 2015), anti-oxidation (Luis et al., 2018) and other effects, it has been studied in numerous disease models. Studies proved that CUR can meaningfully lower the expression of VEGF, CyclinD1, and CDK4 in rats, which was consistent with the previous *in vitro* studies (Huang et al., 2013). On the other hand, a literature discovered that CUR down-regulated TGFβ1 and decreased the amount of Col 1, Col 3 and α-SMA (Wang et al., 2012). The same results were obtained in our experiment. In general, CUR played a protective part in scars. CUR inhibited cell viability and VEGF, Cyclin D1 and CDK4 expressions. Moreover, CUR inhibited TGFβ1-induced soluble collagen, α-SMA, Col 1 and Col 3 levels. In addition, a large number of studies had shown that CUR acted by regulating miRNA. It was discovered that CUR promoted apoptosis of osteosarcoma cells by sponging miR-125a (Chen et al., 2017). Likewise, CUR restrained the tumor proliferation by sponging miR-130a (Dou et al., 2017). So we further studied the relationship between CUR and miRNA in scars.

In recent years, miRNAs have been shown to be involved in the regulation of skin wound repair. For instance, studies had presented miR-181b-5p promoted the proliferation of hypertrophic scars fibroblasts (Liu et al., 2019). It displayed that miR-29 were highly expressed in scars (Bi et al., 2017)and miR-29 mimic can restrained fibroplasia in derma (Gallant-Behm et al., 2018). In this study, we were pleasantly surprised to find that miR-29 and CUR were positively correlated. The miR-29 mimic reduced the expression of VEGF, Cyclin D1 and CDK4. Moreover, it can meaningfully decline the TGFβ1-induced expressions of soluble collagen, α-SMA, Col 1 and Col 3. On the other hand, miR-29 inhibitor reversed the protective functions of CUR on cell proliferation and soluble collagen synthesis. This was similar to the result of Gallant (Gallant-Behm et al., 2018).

Collagen is the main component of the extracellular matrix, Col 1 and Col 3 are mainly present in human skin (Ricard-Blum, 2011). In addition to its support for its own tissue structure, collagen also can regulate cell migration and proliferation (Somaiah et al., 2015). Moreover, Col 1 and Col 3 play an important role in the process of scar formation (Lindsey et al., 2015; Zhao et al., 2018aa; Zhao et al., 2018bb). In this study, we found Col 1 alleviated the CUR-induced

decrease in cell viability and the expression of soluble collagen. Moreover, Col 1 enhanced the ratio of p/t-ERK1/2 and the expression of β-catenin. Meanwhile, si-Col 1 and si-Col 3 declined the ratio of p/t-ERK1/2 and the expression of β-catenin.The ERK1/2 and β-catenin signaling pathways played vital parts in the regulation of scars. Previous studies had reported that ERK1/2 and β-catenin pathways are activated in scars and the two pathways are involved in the pathogenesis of scars (Hahn et al., 2016). Some studies had found that TGFβ1 played a part in scars through ERK1/2 and β-catenin pathways (Deng et al., 2019; Grella et al., 2016). In addition, The research displayed that tetrahydrocurcumin repressed colon tumor by ERK1/2 and β-catenin pathways (Lai et al., 2011). The other research presented miR-29 repressed breast tumor by β-catenin pathway (Rostas et al., 2014). In our study, we discovered that p/t-ERK1/2 ratio and β-catenin expression were reduced after the addition of CUR, and these expression were reversed when transfected miR-29a inhibitor. Otherwise, miR-29a mimic directly declined the ratio of p/t-ERK1/2 and the expression of β-catenin. In short, CUR inhibited scars by ERK1/2 and β-catenin pathways by up-regulating miR-29a.

5. Conclusion

In summary, CUR restrained TGFβ1-induced proliferation and soluble collagen synthesis in NIH-3T3 cells by up-regulation of miR-29a via ERK1/2 and β-catenin signaling pathways. This article afforded a new gist for the clinical treatment of scars.

Declaration of Competing Interest

The authors declare that there are no conflicts of interest.

Acknowledgments

None.

Fundings

This research did not receive any specific grant from funding agencies in the public, commercial, or not-for-profit sectors.

References

Al-Qattan, M.M., Abd-Alwahed, M.M., Shier, M.K., 2018. Effect of TGFβ1 and nAG on astrocyte cultures: a study of astrocyte proliferation and the expression of GFAP, CSPG4, S100B and IL-6. J. Coll. Phys. Surg. Pak. 28, 928–933.
Bi, S., Cao, C., Chai, L.L., Li, S.R., Yang, D.Y., 2017. Regulatory mechanism of miR-29 over TGF-beta1 and COL1 in scar cells. Eur. Rev. Med. Pharmacol. Sci. 21, 2512–2517.
Bondan, E., Cardoso, C., Martins, M.F., 2017. Curcumin decreases astrocytic reaction after gliotoxic injury in the rat brainstem. Arq. Neuropsiquiatr. 75, 546–552.
Carswell, L., Borger, J., 2019. Hypertrophic Scarring Keloids, StatPearls. StatPearls Publishing StatPearls Publishing LLC., Treasure Island (FL).
Chen, P., Wang, H., Yang, F., Chen, H., He, W., Wang, J., 2017. Curcumin promotes osteosarcoma cell death by activating miR-125a/ERRalpha signal pathway. J. Cell. Biochem. 118, 74–81.
Deng, M., Hou, S.Y., Tong, B.D., Yin, J.Y., Xiong, W., 2019. The Smad2/3/4 complex binds miR-139 promoter to modulate TGFbeta-induced proliferation and activation of human Tenon's capsule fibroblasts through the Wnt pathway. J. Cell. Physiol. 234, 13342–13352.
desJardins-Park, H.E., Mascharak, S., Chinta, M.S., Wan, D.C., Longaker, M.T., 2019. The spectrum of scarring in craniofacial wound repair. Front. Physiol. 10, 322.
Devassy, J.G., Nwachukwu, I.D., Jones, P.J., 2015. Curcumin and cancer: barriers to obtaining a health claim. Nutr. Rev. 73, 155–165.
Dou, H., Shen, R., Tao, J., Huang, L., Shi, H., Chen, H., Wang, Y., Wang, T., 2017. Curcumin suppresses the Colon Cancer proliferation by inhibiting Wnt/beta-Catenin pathways via miR-130a. Front. Pharmacol. 8, 877.
Gallant-Behm, C.L., Piper, J., Lynch, J.M., Seto, A.G., Hong, S.J., Mustoe, T.A., Maari, C., Pestano, L.A., Dalby, C.M., Jackson, A.L., Rubin, P., Marshall, W.S., 2018. A MicroRNA-29 mimic (Remlarsen) represses extracellular matrix expression and fibroplasia in the skin. J. Invest. Dermatol.
Gauglitz, G.G., Potschke, J., Clementoni, M.T., 2018. Therapy of scars with lasers. Der Hautarzt; Zeitschrift fur Dermatologie, Venerologie, verwandte Gebiete 69, 17–26.
Grella, A., Kole, D., Holmes, W., Dominko, T., 2016. FGF2 overrides TGFbeta1-Driven integrin ITGA11 expression in human dermal fibroblasts. J. Cell. Biochem. 117, 1000–1008.
Hahn, J.M., McFarland, K.L., Combs, K.A., Supp, D.M., 2016. Partial epithelial-mesenchymal transition in keloid scars: regulation of keloid keratinocyte gene expression by transforming growth factor-beta1. Burns Trauma 4, 30.
Han, B., Fan, J., Liu, L., Tian, J., Gan, C., Yang, Z., Jiao, H., Zhang, T., Liu, Z., Zhang, H., 2019. Adipose-derived mesenchymal stem cells treatments for fibroblasts of fibrotic scar via downregulating TGF-beta1 and Notch-1 expression enhanced by photobiomodulation therapy. Lasers Med. Sci. 34, 1–10.
Huang, C.Z., Huang, W.Z., Zhang, G., Tang, D.L., 2013. In vivo study on the effects of curcumin on the expression profiles of anti-tumour genes (VEGF, CyclinD1 and CDK4) in liver of rats injected with DEN. Mol. Biol. Rep. 40, 5825–5831.
Jia, S., Xie, P., Hong, S.J., Galiano, R., Singer, A., Clark, R.A., Mustoe, T.A., 2014. Intravenous curcumin efficacy on healing and scar formation in rabbit ear wounds under nonischemic, ischemic, and ischemia-reperfusion conditions. Wound Repair Regen. 22, 730–739.
Lai, C.S., Wu, J.C., Yu, S.F., Badmaev, V., Nagabhushanam, K., Ho, C.T., Pan, M.H., 2011. Tetrahydrocurcumin is more effective than curcumin in preventing azoxymethane-induced colon carcinogenesis. Mol. Nutr. Food Res. 55, 1819–1828.
Lelli, D., Sahebkar, A., Johnston, T.P., Pedone, C., 2017. Curcumin use in pulmonary diseases: state of the art and future perspectives. Pharmacol. Res. 115, 133–148.
Lichtman, M.K., Otero-Vinas, M., Falanga, V., 2016. Transforming growth factor beta (TGF-beta) isoforms in wound healing and fibrosis. Wound Repair Regen. 24, 215–222.
Lindsey, M.L., Iyer, R.P., Zamilpa, R., Yabluchanskiy, A., DeLeon-Pennell, K.Y., Hall, M.E., Kaplan, A., Zouein, F.A., Bratton, D., Flynn, E.R., 2015. A novel collagen matricryptin reduces left ventricular dilation post-myocardial infarction by promoting scar formation and angiogenesis. J. Am. Coll. Cardiol. 66, 1364–1374.
Liu, B., Guo, Z., Gao, W., 2019. miR-181b-5p promotes proliferation and inhibits apoptosis of hypertrophic scar fibroblasts through regulating the MEK/ERK/p21 pathway. Exp. Ther. Med. 17, 1537–1544.
Luis, P.B., Boeglin, W.E., Schneider, C., 2018. Thiol reactivity of curcumin and its oxidation products. Chem. Res. Toxicol. 31, 269–276.
Ogawa, R., 2019. Surgery for scar revision and reduction: from primary closure to flap surgery. Burns Trauma 7, 7.
Ricard-Blum, S., 2011. The collagen family. Cold Spring Harb. Perspect. Biol. 3, a004978.
Rostas 3rd, J.W., Pruitt, H.C., Metge, B.J., Mitra, A., Bailey, S.K., Bae, S., Singh, K.P., Devine, D.J., Dyess, D.L., Richards, W.O., Tucker, J.A., Shevde, L.A., Samant, R.S., 2014. microRNA-29 negatively regulates EMT regulator N-myc interactor in breast cancer. Mol. Cancer 13, 200.
Saidi, A., Kasabova, M., Vanderlynden, L., Wartenberg, M., Kara-Ali, G.H., Marc, D., Lecaille, F., Lalmanach, G., 2019. Curcumin inhibits the TGF-beta1-dependent differentiation of lung fibroblasts via PPARgamma-driven upregulation of cathepsins B and L. Sci. Rep. 9, 491.
Somaiah, C., Kumar, A., Mawrie, D., Sharma, A., Patil, S.D., Bhattacharyya, J., Swaminathan, R., Jaganathan, B.G., 2015. Collagen promotes higher adhesion, survival and proliferation of mesenchymal stem cells. PloS One 10, e0145068.
Tu, L., Huang, Q., Fu, S., Liu, D., 2018. Aberrantly expressed long noncoding RNAs in hypertrophic scar fibroblasts in vitro: a microarray study. Int. J. Mol. Med. 41, 1917–1930.
Vecchi Brumatti, L., Marcuzzi, A., Tricarico, P.M., Zanin, V., Girardelli, M., Bianco, A.M., 2014. Curcumin and inflammatory bowel disease: potential and limits of innovative treatments. Molecules (Basel, Switzerland) 19, 21127–21153.
Wang, N.P., Wang, Z.F., Tootle, S., Philip, T., Zhao, Z.Q., 2012. Curcumin promotes cardiac repair and ameliorates cardiac dysfunction following myocardial infarction. Br. J. Pharmacol. 167, 1550–1562.
Xiao, A., Ettefagh, L., 2019. Laser Revision Of Scars, StatPearls. StatPearls Publishing StatPearls Publishing LLC., Treasure Island (FL).
Xiao, L., He, H., Ma, L., Da, M., Cheng, S., Duan, Y., Wang, Q., Wu, H., Song, X., Duan, W., Tian, Z., Hou, Y., 2017. Effects of miR-29a and miR-101a expression on myocardial interstitial collagen generation after aerobic exercise in myocardial-infarcted rats. Arch. Med. Res. 48, 27–34.
Yuan, J., Botchway, B.O.A., Zhang, Y., Tan, X., Wang, X., Liu, X., 2019. Curcumin can improve spinal cord injury by inhibiting TGF-beta-SOX9 signaling pathway. Cell. Mol. Neurobiol.
Yuan, J., Liu, W., Zhu, H., Chen, Y., Zhang, X., Li, L., Chu, W., Wen, Z., Feng, H., Lin, J., 2017. Curcumin inhibits glial scar formation by suppressing astrocyte-induced inflammation and fibrosis in vitro and in vivo. Brain Res. 1655, 90–103.
Yuan, J., Zou, M., Xiang, X., Zhu, H., Chu, W., Liu, W., Chen, F., Lin, J., 2015. Curcumin improves neural function after spinal cord injury by the joint inhibition of the intracellular and extracellular components of glial scar. J. Surg. Res. 195, 235–245.
Zhang, Q., Guo, B., Hui, Q., Chang, P., Tao, K., 2018. miR-137 inhibits proliferation and metastasis of hypertrophic scar fibroblasts via targeting pleiotrophin. Cell. Physiol. Biochem. 49, 985–995.
Zhao, M.J., Chen, S.Y., Qu, X.Y., Abdul-Fattah, B., Lai, T., Xie, M., Wu, S.D., Zhou, Y.W., Huang, C.Z., 2018a. Increased Cthrc1 activates normal fibroblasts and suppresses keloid fibroblasts by inhibiting TGF-beta/Smad signal pathway and modulating YAP subcellular location. Curr. Med. Sci. 38, 894–902.
Zhao, X., Song, W., Chen, Y., Liu, S., Ren, L., 2018b. Collagen-based materials combined with microRNA for repairing cornea wounds and inhibiting scar formation. Biomater. Sci. 7, 51–62.
Zhou, S., Zhang, S., Shen, H., Chen, W., Xu, H., Chen, X., Sun, D., Zhong, S., Zhao, J., Tang, J., 2017. Curcumin inhibits cancer progression through regulating expression of microRNAs. Tumour Biol. 39, 1010428317691680.